Scaled geometric Brownian motion features sub- or superexponential ensemble-averaged, but linear time-averaged mean-squared displacements

Andrey G. Cherstvy [1,2,*] Deepak Vinod [1,†] Erez Aghion [3,‡] Igor M. Sokolov [4,§] and Ralf Metzler [1,‖]

[1] *Institute for Physics & Astronomy, University of Potsdam, 14476 Potsdam-Golm, Germany*

[2] *Institut für Physik, Humboldt-Universität zu Berlin, 12489 Berlin, Germany*

[3] *Max Planck Institute for the Physics of Complex Systems, 01187 Dresden, Germany*

[4] *Institut für Physik and IRIS Adlershof, Humboldt-Universität zu Berlin, 12489 Berlin, Germany*

(Received 16 March 2021; accepted 24 May 2021; published 15 June 2021)

Various mathematical Black-Scholes-Merton-like models of option pricing employ the paradigmatic stochastic process of geometric Brownian motion (GBM). The innate property of such models and of real stock-market prices is the roughly exponential growth of prices with time [on average, in crisis-free times]. We here explore the ensemble- and time averages of a multiplicative-noise stochastic process with power-law-like time-dependent volatility, $\sigma(t) \sim t^{\alpha}$, named scaled GBM (SGBM). For SGBM, the mean-squared displacement (MSD) computed for an ensemble of statistically equivalent trajectories can grow faster than exponentially in time, while the time-averaged MSD (TAMSD)—based on a sliding-window averaging along a single trajectory—is always linear at short lag times Δ. The proportionality factor between these the two averages of the time series is Δ/T at short lag times, where T is the trajectory length, similarly to GBM. This discrepancy of the scaling relations and pronounced nonequivalence of the MSD and TAMSD at $\Delta/T \ll 1$ is a manifestation of weak ergodicity breaking for standard GBM and for SGBM with $\sigma(t)$-modulation, the main focus of our analysis. The analytical predictions for the MSD and mean TAMSD for SGBM are in quantitative agreement with the results of stochastic computer simulations.

DOI: 10.1103/PhysRevE.103.062127

I. INTRODUCTION

Pioneered by Bachelier [1] and Bronzin [2] more than a century ago, price fluctuations on stock markets are believed to follow random walks and "arithmetic" Brownian motion (BM) in particular. The widely recognized Black-Scholes-Merton (BSM) model [3–5]—employing instead "exponential" or geometric BM (GBM) as the exponentially growing solution of the multiplicative-noise stochastic differential equation [6]—has been shaping the field of financial mathematics for decades. The magnitude of price fluctuations over a certain time span yields volatility of a stock or asset, σ. This concept—of constant, time-dependent, or stochastic volatility—is crucial for the detailed mathematical modeling and general understanding of the underlying principles of functioning of financial markets [7–11].

One source of deficiencies and imperfections of standard BSM-model-based predictions stems from assuming a constant, time-invariant volatility σ yielding log-normally distributed prices of an option at expiration (not always true). Numerous modifications of the BSM model were proposed—to account for time-varying, stochastic or fluctuating volatilities [8–10,12–16], anticorrelations of changes in price and in volatility [17], alternative diffusion processes [11,18,19], price-dependent volatility [20–22], jump diffusion [5,14,23], and other relevant effects—to make such modified-GBM-based models more applicable to the quantitative analysis of real financial data. GBM modifications for subdiffusive dynamics [24–26] and with fractional BM [27] were developed.

The concept of stochastic volatility, e.g., involves a separate stochastic equation [12] for a time- and price-value-dependent volatility, $\sigma(X,t)$. As another example, the diffusion model of constant elasticity of variance (CEV) is based on the volatility dependent as a power law on price [20–22],

$$\sigma(X) \sim X^{\gamma}, \tag{1}$$

with the square-root process realized at $\gamma = -1/2$ [18]. In the physics literature, diffusion models with a space-dependent power-law-varying diffusivity were proposed recently as heterogeneous diffusion processes [28–33].

During periods of high volatilities the trading situation on stock markets can change rapidly and dramatically, also with certain systematic trends in the volatility behavior, e.g., during a systematic development of a specific stock. The response of a market to incoming news and financial announcements can also imprint characteristic patterns in the volatility-variation function with time. Option-valuation models with deterministic volatility function (of time and price)

*a.cherstvy@gmail.com
†ugdeepakv@gmail.com
‡erezagh5@gmail.com
§igor.sokolov@physik.hu-berlin.de
‖rmetzler@uni-potsdam.de

were thus developed [34,35]. Such systematic power-law variation of volatility in time were detected, e.g., in the analysis of the intraday dynamics of foreign-exchange markets [36–39]. Specifically, the increments of returns of the Euro-Dollar rate, $\log[P(t+\delta t)/P(t)]$ with $\delta t = 10$ min, were shown to be nonstationary, with their standard deviation $\bar{\sigma}(t)$ revealing a clear daily periodicity [37]. On a timescale of several hours, the time regions of both increasing and decreasing $\bar{\sigma}(t)$ of a power-law form were detected. For instance, in the first 3 hours after 9 AM New-York time for the Euro-Dollar pair the power-law variation $\bar{\sigma}(t) \sim t^{-0.13}$ was found [37]. These observations for real financial markets motivated this theoretical study.

Below, we consider scaled GBM (SGBM) with volatility varying as a power law in time,

$$\sigma(t) = \sigma_\alpha t^\alpha. \tag{2}$$

An analog of SGBM for a nonmultiplicative case is scaled BM (SBM), a nonstationary nonergodic process with the time-dependent diffusivity of the form [30,40–46],

$$D(t) \sim t^{\tilde{\alpha}-1}. \tag{3}$$

SBM yields anomalous scaling for the mean-squared displacement (MSD), while the time-averaged MSD (TAMSD) grows linearly with the lag time. We emphasize that the scaled "exponential" BM (or SGBM) should not be mixed with the process of exponential SBM introduced recently [46]. Below, we compute the MSD and mean TAMSD of SGBM and compare them to the results for conventional GBM [47,48].

This paper—targeting, primarily, the community of stochastic processes and, secondarily, that of financial mathematics—is structured as follows. We start with definitions and observables in Sec. II. In Sec. III the results for the MSD and mean TAMSD of canonical GBM are presented for a reference. In Sec. IV we compute the same for SGBM and show that their functional forms and the MSD-to-TAMSD ratio are similar. Our analytical predictions agree closely with findings from stochastic computer simulations, see Sec. V. We draw conclusions in Sec. VI and present auxiliary figures in Appendix A, whereas other forms of $\sigma(t)$ are outlined in Appendix B.

II. DEFINITIONS AND OBSERVABLES

For the financial time series, the concept of "ensemble averaging" is not applicable due to the innate irreproducibility of price-evolution "experiments." Thus, single-trajectory-based characteristics, such as the TAMSD [49]

$$\overline{\delta^2(\Delta)} = \frac{1}{T-\Delta}\int_0^{T-\Delta} [X(t+\Delta) - X(t)]^2 dt, \tag{4}$$

are more informative and relevant variables. Here Δ is the lag time and T is the length of the time series. Hereafter, averaging over noise realizations is denoted by the angular brackets, while time averaging is shown by the overline. Averaging over N (independent and statistically equivalent) TAMSD realizations yields the mean TAMSD (arithmetic mean),

$$\langle\overline{\delta^2(\Delta)}\rangle = \frac{1}{N}\sum_{i=1}^{N}\overline{\delta_i^2(\Delta)}. \tag{5}$$

Ergodicity necessitates the MSD-to-TAMSD equivalence at $\Delta/T \ll 1$ for long time series [49], a feature of complete sampling of accessible states in the phase-space. The inherently nonstationary nature of financial time series [37,39,50] questions the existence of an "equilibrium ensemble" (constructed, e.g., from equal-length nonoverlapping segments of a long trajectory), the appropriateness of fixed-parameter sliding-window-based averaging approaches, and the ergodic hypothesis itself [48,51,52].

III. GBM: THEORETICAL RESULTS

A. MSD

The process of standard GBM $X(t)$ is the solution of the stochastic differential equation

$$dX(t) = \mu X(t)dt + \sigma X(t)dW(t), \tag{6}$$

where $X(t)$ is the value at time t, μ is the drift, and σ is the volatility (both assumed to be constant for now). We consider Eq. (6) below in Îto interpretation, typical for the mathematical literature in economics. Here $dW(t)$ are increments of the Wiener process, defined via the integral of white Gaussian zero-mean noise $\xi(t)$ as

$$W(t) = \int_0^t \xi(t')dt'. \tag{7}$$

In Eq. (6) the noise enters "multiplicatively" with the process itself, i.e., $\sigma X(t) \times dW(t)$. The variation of stock-market prices with time, starting with an initial value

$$X(t=0) > 0, \tag{8}$$

can be described using Îto's lemma [8,10]. Equation (6) yields an exponentially growing GBM process of the form

$$X(t) = X(0)e^{(\mu-\sigma^2/2)t+\sigma W(t)}. \tag{9}$$

Using the associated log-normal distribution,

$$p(X(t),t) = \frac{\exp\left(-\frac{\{\log[X(t)/X(0)]-(\mu-\sigma^2/2)t\}^2}{2\sigma^2 t}\right)}{\sqrt{2\pi\sigma^2 t[X(t)]^2}}, \tag{10}$$

one obtains for GBM the mean $\langle X_{\rm GBM}(t)\rangle = X(0)e^{\mu t}$, the second moment

$$\left\langle X_{\rm GBM}^2(t)\right\rangle = [X(0)]^2 e^{(2\mu+\sigma^2)t}, \tag{11}$$

and the variance

$$\begin{aligned}&\langle (X_{\rm GBM}(t) - \langle X_{\rm GBM}(t)\rangle)^2\rangle \\ &= \int_0^\infty (X(t) - \langle X(t)\rangle)^2 p(X(t),t)\,dX(t) \\ &= [X(0)]^2 e^{2\mu t}(e^{\sigma^2 t} - 1).\end{aligned} \tag{12}$$

At $\mu = 0$ one gets $\langle X_{\rm GBM}^2(T)\rangle = [X(0)]^2 e^{\sigma^2 T}$. With the probability distribution of the Wiener process,

$$p(W(t),t) = \exp[-W(t)^2/(2t)]/\sqrt{2\pi t}, \tag{13}$$

via averaging (9) over realizations of $W(t)$, one gets the same expressions for the moments.

B. TAMSD

Using the two-point transition probability for the Wiener process ($t_2 < t_1$),

$$p_{12}(W_1,t_1;W_2,t_2)=\exp\left[-\frac{(W_1-W_2)^2}{2(t_1-t_2)}\right]\Big/\sqrt{2\pi(t_1-t_2)}, \tag{14}$$

the mean TAMSD of GBM (9) becomes [47,48]

$$\left\langle\overline{\delta^2_{\rm GBM}(\Delta)}\right\rangle=\frac{[X(0)]^2[1-2e^{\mu\Delta}+e^{\Delta(2\mu+\sigma^2)}]}{T-\Delta}\times\frac{e^{(2\mu+\sigma^2)(T-\Delta)}-1}{2\mu+\sigma^2}. \tag{15}$$

Here the averaging of

$$\langle[X(t+\Delta)-X(t)]^2\rangle=\langle X^2(t+\Delta)\rangle+\langle X^2(t)\rangle-2\langle X(t+\Delta)X(t)\rangle \tag{16}$$

in the integrand of Eq. (4) was performed using Eqs. (13) and (15). As with no drift

$$\left\langle\overline{\delta^2_{\rm GBM}(\Delta)}\right\rangle=\frac{[X(0)]^2(e^{\sigma^2\Delta}-1)}{T-\Delta}\frac{e^{\sigma^2(T-\Delta)}-1}{\sigma^2}, \tag{17}$$

for short lag times ($\Delta\ll T$ and $\sigma^2\Delta\ll 1$) and long trajectories ($\sigma^2T\gg 1$) one gets

$$\left\langle\overline{\delta^2_{\rm GBM}(\Delta)}\right\rangle\approx[X(0)]^2(e^{\sigma^2T}-1)\frac{\Delta}{T}\approx\langle[X_{\rm GBM}(T)-\langle X_{\rm GBM}(T)\rangle]^2\rangle\frac{\Delta}{T}\sim\left\langle X^2_{\rm GBM}(T)\right\rangle\frac{\Delta}{T}. \tag{18}$$

Therefore, for GBM the mean TAMSD and MSD are proportional with the factor Δ/T, the fact also confirmed by computer simulations, see Ref. [48] and below.

IV. SGBM: THEORETICAL RESULTS

A. MSD

For a deterministic time-dependent volatility $\sigma(t)$, starting with the analog of Eq. (6) with σ being replaced by $\sigma(t)$ and after using the Îto lemma, the solution of the SGBM equation,

$$d[\log(X(t))]=[\mu-\sigma^2(t)/2]dt+\sigma(t)dW(t), \tag{19}$$

is similar to Eq. (9) (see Sec. 2.2.1 of Ref. [10] and Eq. (6.34) in Sec. 5.6 of Ref. [7]), namely

$$X(T)=X(t)e^{\mu(T-t)-\int_t^T\sigma^2(t')dt'/2+\int_t^T\sigma(t')dW(t')}. \tag{20}$$

Here t and T are the initial and final times of the process. This process stays log-normally distributed, with its mean and variance redefined in terms of the *time-averaged* squared volatility [10] [denoted below by a wide tilde, to distinguish it from time-averaging in Eq. (4)],

$$\widetilde{\sigma^2(T,t)}=\frac{1}{T-t}\int_t^T\sigma^2(t')dt'. \tag{21}$$

The "effective volatility" is a quadratic mean of $\sigma(t)$ over the lifetime of an option.

In analogy to SBM, for SGBM we set the volatility being a power-law function, $\sigma(t)=\sigma_\alpha t^\alpha$, where σ_α is the volatility magnitude (with physical dimensions $[\sigma_\alpha]=1/{\rm s}^{\alpha+1/2}$). Positive (negative) values of the exponent α describe the MSD growing faster (slower) compared to that for GBM. From (21), after setting $t=0$, the dependence of the squared-averaged volatility on time is

$$\widetilde{\sigma^2(t)}=\frac{1}{t}\frac{\sigma_\alpha^2t^{2\alpha+1}}{2\alpha+1}. \tag{22}$$

The range of exponents α is limited below to

$$\alpha>-1/2, \tag{23}$$

see the reasoning in Sec. VI. For the second moment and the variance of SGBM, using the log-normal distribution analogous to (10) for GBM,

$$p(X(t),t)=\frac{\exp\left(-\frac{\{\log[X(t)/X(0)]-[\mu-\widetilde{\sigma^2(t)}/2]t\}^2}{2\widetilde{\sigma^2(t)}t}\right)}{\sqrt{2\pi\widetilde{\sigma^2(t)}t[X(t)]^2}}, \tag{24}$$

we get

$$\left\langle X^2_{\rm SGBM}(t)\right\rangle=[X(0)]^2e^{2\mu t}e^{\frac{\sigma_\alpha^2t^{2\alpha+1}}{2\alpha+1}} \tag{25}$$

and

$$\langle(X_{\rm SGBM}(t)-\langle X_{\rm SGBM}(t)\rangle)^2\rangle=[X(0)]^2e^{2\mu t}\left(e^{\frac{\sigma_\alpha^2t^{2\alpha+1}}{2\alpha+1}}-1\right). \tag{26}$$

As expected, these expressions turn into expressions (11) and (12) for standard GBM upon a formal substitution σ^2 to $\widetilde{\sigma^2(t)}$. Thus, for SGBM with the volatility growing in time (at $\alpha>0$) expressions (25) and (26) yield a faster-than-exponential (superexponential) growth of the MSD, as compared to the exponential one for GBM. The ratio of the second moments for SGBM and GBM at time t is

$$\frac{\left\langle X^2_{\rm SGBM}(t)\right\rangle}{\left\langle X^2_{\rm GBM}(t)\right\rangle}\approx\frac{e^{\frac{\sigma_\alpha^2t^{2\alpha+1}}{2\alpha+1}}}{e^{\sigma_0^2t}}. \tag{27}$$

Therefore, if one neglects a possible time-dependence of the volatility, then the MSD predictions acquire exponentially growing deviations at long times.

B. TAMSD

1. Derivation 1

The integrands of the mean TAMSD of SGBM at $\mu=0$ can be expressed, utilizing the approximate statistical independence of $2X(t)$ and $X(t+\Delta)-X(t)$ at short lag times, as

$$\langle[X(t+\Delta)-X(t)]^2\rangle\approx\langle X^2(t+\Delta)\rangle-\langle X^2(t)\rangle. \tag{28}$$

Evaluating the TAMSD integral using Eq. (25) (in the absence of drift, $\mu=0$),

$$\left\langle\overline{\delta^2_{\rm SGBM}(\Delta)}\right\rangle=\frac{\int_0^{T-\Delta}\langle[X_{\rm SGBM}(t+\Delta)-X_{\rm SGBM}(t)]^2\rangle dt}{T-\Delta}\approx\frac{[X(0)]^2}{T-\Delta}\int_0^{T-\Delta}\left[e^{\frac{\sigma_\alpha^2(t+\Delta)^{2\alpha+1}}{2\alpha+1}}-e^{\frac{\sigma_\alpha^2t^{2\alpha+1}}{2\alpha+1}}\right]dt, \tag{29}$$

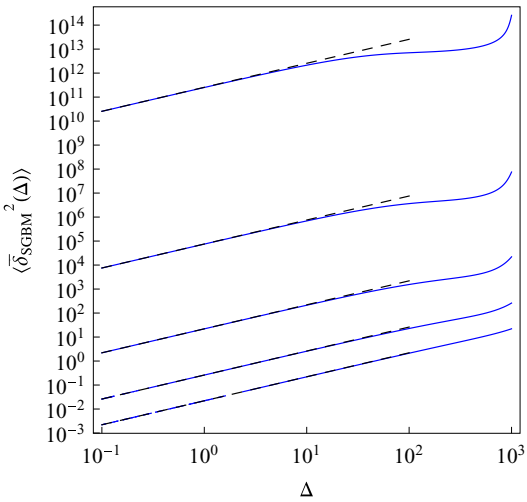

FIG. 1. Variation of the mean TAMSD of SGBM with the lag time (30) and the short-lag-time asymptote (32), plotted for a varying SGBM parameter $\alpha = \{-0.1, -0.05, 0, 0.05, 0.1\}$ (for the curves from bottom to top). Other parameters are $X(0) = 1$, $T = 10^3$, and $\sigma_\alpha = 10^{-1}$ (given without physical units hereafter).

one arrives at

$$\overline{\langle\delta^2_{\rm SGBM}(\Delta)\rangle} = \frac{[X(0)]^2\left(-\frac{\sigma_\alpha^2}{1+2\alpha}\right)^{\frac{2\alpha}{1+2\alpha}}}{\sigma_\alpha^2(T-\Delta)} \times \left(\Gamma\left[\frac{1}{1+2\alpha}\right] - \Gamma\left[\frac{1}{1+2\alpha}, -\frac{\sigma_\alpha^2\Delta^{1+2\alpha}}{1+2\alpha}\right] + \Gamma\left[\frac{1}{1+2\alpha}, -\frac{\sigma_\alpha^2 T^{1+2\alpha}}{1+2\alpha}\right] - \Gamma\left[\frac{1}{1+2\alpha}, -\frac{\sigma_\alpha^2(T-\Delta)^{1+2\alpha}}{1+2\alpha}\right]\right), \tag{30}$$

where $\Gamma(x)$ is the Gamma function and $\Gamma(a, z)$ is the (upper) incomplete Gamma function,

$$\Gamma(a, z) = \int_z^\infty t^{a-1}e^{-t}dt. \tag{31}$$

For short lag times and long trajectories, at $\Delta \ll T$, the leading term in the expansion of (30) yields a linear asymptote

$$\overline{\langle\delta^2_{\rm SGBM}(\Delta)\rangle} \approx [X(0)]^2\left(e^{\frac{\sigma_\alpha^2 T^{2\alpha+1}}{2\alpha+1}} - 1\right)\frac{\Delta}{T}, \tag{32}$$

see Fig. 1. The region of short lag times is our main focus when considering the mean TAMSD. The MSD and the mean TAMSD for SGBM are, therefore, similarly to standard GBM, connected at short lag times via the proportionality factor of (Δ/T), namely

$$\overline{\langle\delta^2_{\rm SGBM}(\Delta)\rangle} \approx \langle X^2_{\rm SGBM}(T)\rangle \times \frac{\Delta}{T}. \tag{33}$$

Thus, despite a superexponential growth of the MSD for a volatility growing in time [at $\alpha > 0$, see Eqs. (25) and (26)], the mean TAMSD of SGBM increases linearly with the lag time in the limit $\Delta/T \ll 1$, see Eq. (33). The increased magnitude of the MSD of SGBM at $\alpha > 0$ acts solely as a larger prefactor for the mean TAMSD. This is the main conclusion of TAMSD derivations for SGBM, Last, both for GBM (18) and SGBM (33) the MSD and the mean TAMSD are equal at the terminal point of the trajectory, at $\Delta = T$, as they should [49].

2. Derivation 2

A more rigorous derivation of the mean TAMSD of SGBM with nonzero drift is as follows. The stochastic integral in the SGBM equation, after employing Îto lemma, Eq. (19), is equal in distribution (denoted as $\overset{\rm dist.}{=}$ below) to

$$\int_{t_1}^{t_2}\sigma(t')dW(t') \overset{\rm dist.}{=} w\sqrt{\int_{t_1}^{t_2}[\sigma(t')]^2dt'}. \tag{34}$$

To prove it, we use a representation of BM as the sum of (dimensionless) random numbers w_n taken from the probability density

$$p(w) = e^{-w^2/2}/\sqrt{2\pi}, \tag{35}$$

namely

$$W(t) = \sum_{n=0}^{t/dt} w_n. \tag{36}$$

As the variance of BM grows linearly with time, the relation (34) (in the continuous limit) can be proved via the discrete summation [53]

$$\int_0^t \sigma(t')dW(t') = \sum_{n=0}^{t/dt-1}\sigma(n\times dt)\{W[(n+1)dt] - W(n\times dt)\} = \sqrt{dt}\sum_{n=0}^{t/dt-1}\sigma(n\times dt)w_n \overset{\rm dist.}{=} w\sqrt{dt}\sqrt{\sum_{n=0}^{t/dt-1}\sigma^2(n\times dt)} \overset{n\to\infty}{=} w\sqrt{dt}\sqrt{\frac{1}{dt}\int_0^t\sigma^2(t')dt'}. \tag{37}$$

Here the values of the volatility $\sigma(t)$ are taken at the start of the nth interval in this discrete sum in order to comply with Îto's representation (prepoint stochastic convention).

The general expression for SGBM $X_w(t)$ then becomes

$$X_w(t_2) \overset{\rm dist.}{=} X_w(t_1)\times e^{\mu(t_2-t_1)-\frac{1}{2}\int_{t_1}^{t_2}\sigma(t')^2dt' + w\sqrt{\int_{t_1}^{t_2}[\sigma(t')]^2dt'}}, \tag{38}$$

that, after using the explicit dependence of volatility on time (2), turns into

$$X_w(t_2) \overset{\rm dist.}{=} X_w(t_1)e^{\mu(t_2-t_1) - \frac{\sigma_\alpha^2\left(t_2^{2\alpha+1}-t_1^{2\alpha+1}\right)}{2(2\alpha+1)} + \frac{w\sigma_\alpha\sqrt{t_2^{2\alpha+1}-t_1^{2\alpha+1}}}{\sqrt{2\alpha+1}}}. \tag{39}$$

For $t_2 = t$ and $t_1 = 0$, using the distribution function (35), one obtains expression (25) for the MSD of SGBM (39), namely

$$\langle X_w^2(t)\rangle = \int_{-\infty}^{+\infty}X_w^2(t)p(w)dw = [X(0)]^2e^{2\mu t}e^{\frac{\sigma_\alpha^2 t^{2\alpha+1}}{2\alpha+1}}. \tag{40}$$

For the correlation term in Eq. (16), expressing $X_w(t+\Delta)$ via $X_w(t)$, one arrives at

$$\langle X_w(t+\Delta)X_w(t)\rangle \overset{\text{dist.}}{=} \langle X_w^2(t)\rangle e^{\mu\Delta} e^{-\frac{\sigma_\alpha^2[(t+\Delta)^{2\alpha+1}-t^{2\alpha+1}]}{2(2\alpha+1)}} \times \int_{-\infty}^{+\infty} e^{\frac{w\sigma_\alpha\sqrt{(t+\Delta)^{2\alpha+1}-t^{2\alpha+1}}}{\sqrt{2\alpha+1}}} p(w)dw = \langle X_w^2(t)\rangle e^{\mu\Delta}, \quad (41)$$

that yields for the integrand of the mean TAMSD

$$\langle [X_w(t+\Delta)-X_w(t)]^2\rangle = [X(0)]^2 e^{2\mu t}\left[e^{2\mu\Delta}e^{\frac{\sigma_\alpha^2(t+\Delta)^{2\alpha+1}}{2\alpha+1}} - 2e^{\mu\Delta}e^{\frac{\sigma_\alpha^2 t^{2\alpha+1}}{2\alpha+1}} + e^{\frac{\sigma_\alpha^2 t^{2\alpha+1}}{2\alpha+1}}\right]. \quad (42)$$

With no drift, this gives the same TAMSD integrand and the leading-order expansion at short lag times as in (30) supporting the validity of approximation (28) in this limit. Naturally, for $\alpha = 0$ expression (42) turns into the TAMSD integrand (15) for standard GBM [48], that is

$$\frac{\langle [X_w(t+\Delta)-X_w(t)]^2\rangle}{[X(0)]^2} = e^{(\sigma_0^2+2\mu)t}\left[e^{(\sigma_0^2+2\mu)\Delta} - 2e^{\mu\Delta} + 1\right]. \quad (43)$$

3. *Visualization of theoretical results*

The evolution of the TAMSD for SGBM with lag time is shown in Fig. 1. We expectedly observe an increase of the mean-TAMSD magnitude with the growing exponent α. For larger α, when the condition $\sigma_\alpha^2 T^{2\alpha+1} \gg 1$ holds and the TAMSD magnitude (32) grows exponentially, a *plateaulike regime* of the mean TAMSD of SGBM at intermediate lag time can emerge, see Figs. 1 and 7. In this regime the second-order term for the expansion (32) starts to be non-negligible. The characteristic lag time $\Delta^\star$ after which the TAMSD plateau is realized can be assessed via equating the first and second term of the TAMSD expansion. This yields

$$\Delta^\star \sim \frac{2T}{\sigma_\alpha^2 T^{2\alpha+1}} \quad (44)$$

and a "transient" TAMSD plateau with the height

$$\langle\overline{\delta^2_{\text{SGBM}}(\Delta)}\rangle_{\text{pl}} \sim \frac{1}{2}[X(0)]^2\left(\frac{\Delta^\star}{T}\right)e^{\frac{\sigma_\alpha^2 T^{2\alpha+1}}{2\alpha+1}}. \quad (45)$$

In the opposite limit of large values of the lag time, at $\Delta \to T$, the Taylor expansion of (30) gives

$$\frac{\langle\overline{\delta^2_{\text{SGBM}}(\Delta)}\rangle}{[X(0)]^2} \sim \left(e^{\frac{\sigma_\alpha^2 T^{2\alpha+1}}{2\alpha+1}} - 1\right) - e^{\frac{\sigma_\alpha^2 T^{2\alpha+1}}{2\alpha+1}}\left(\frac{\sigma_\alpha^2 T^{2\alpha}}{2}\right)(T-\Delta). \quad (46)$$

The ratio of the TAMSDs for SGBM and GBM, computed at short lag times (where the TAMSD gives the most statistically accurate averaging [49]), given by

$$\frac{\langle\overline{\delta^2_{\text{SGBM}}(\Delta)}\rangle}{\langle\overline{\delta^2_{\text{GBM}}(\Delta)}\rangle} \approx \frac{e^{\frac{\sigma_\alpha^2 T^{2\alpha+1}}{2\alpha+1}} - 1}{e^{\sigma_0^2 T} - 1}, \quad (47)$$

grows with exponent α in almost the entire range, as demonstrated in Fig. 2. The functional dependence (47) is similar to that of the ratio of the MSDs in Eq. (27). In the region of parameters when both exponential functions in (47) can be expanded, at

$$\sigma_\alpha^2 T^{2\alpha+1} \ll 1 \text{ and } \sigma_0^2 T \ll 1, \quad (48)$$

this ratio becomes

$$\frac{\langle\overline{\delta^2_{\text{SGBM}}(\Delta)}\rangle}{\langle\overline{\delta^2_{\text{GBM}}(\Delta)}\rangle} \sim \frac{T^{2\alpha}}{2\alpha+1}. \quad (49)$$

This asymptote (independent on the volatility value) describes the actual dependence for progressively larger values of α as the magnitudes of σ_α and σ_0 decrease, as Fig. 2 illustrates. We observe that, as the volatility values decrease, the short-lag-time ratio of the TAMSDs follows the asymptote (49) up to large values of scaling exponent α. When $\sigma_0^2 T \gg 1$ and $\sigma_\alpha^2 T^{2\alpha+1} \ll 1$, the TAMSD ratio (47) at short lag times simplifies to

$$\frac{\langle\overline{\delta^2_{\text{SGBM}}(\Delta)}\rangle}{\langle\overline{\delta^2_{\text{GBM}}(\Delta)}\rangle} \sim \frac{\sigma_\alpha^2 T^{2\alpha+1}}{(2\alpha+1)e^{\sigma_0^2 T}}. \quad (50)$$

As $\alpha \to -1/2$ (from the right), the ratio of TAMSDs (47) rapidly increases: the squared time-averaged volatility (22) diverges in this limit that produces an *unexpected* growth of the TAMSDs' ratio (47) near the "critical point" $\alpha = -1/2$, see Fig. 2.

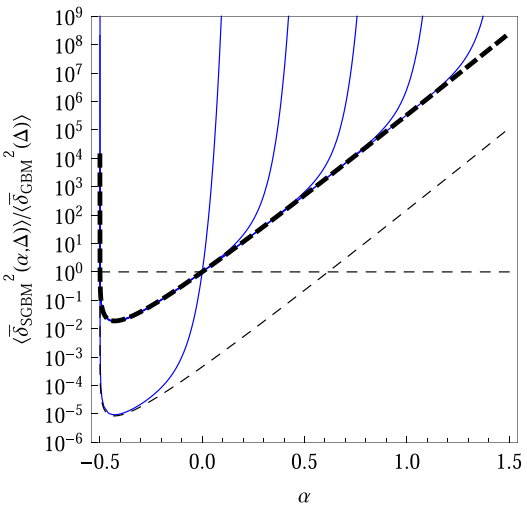

FIG. 2. Ratio of the mean TAMSDs of SGBM and GBM given by Eq. (47), for σ_α and σ_0 taking the values $\{10^{-5}, 10^{-4}, 10^{-3}, 10^{-2}, 10^{-1}\}$ (for the curves from right to left), plotted for varying exponents α at short lag times, $\Delta/T \ll 1$. The functional dependence in the limit of small volatilities given by Eq. (49) is the thick dashed curve, while Eq. (50) is shown as the lower dashed curve. Other parameters are the same as in Fig. 1.

V. SGBM: SIMULATION RESULTS

A. Simulation scheme

From Eq. (19), the infinitesimal increments of SGBM at time t depend on the time-local volatility $\sigma(t)$ and are being driven by the increments of $W(t)$. The latter are modeled using the unit-variance and zero-mean normal distribution as

$$dW(t) \sim \mathcal{N}(0,1) \times dt. \quad (51)$$

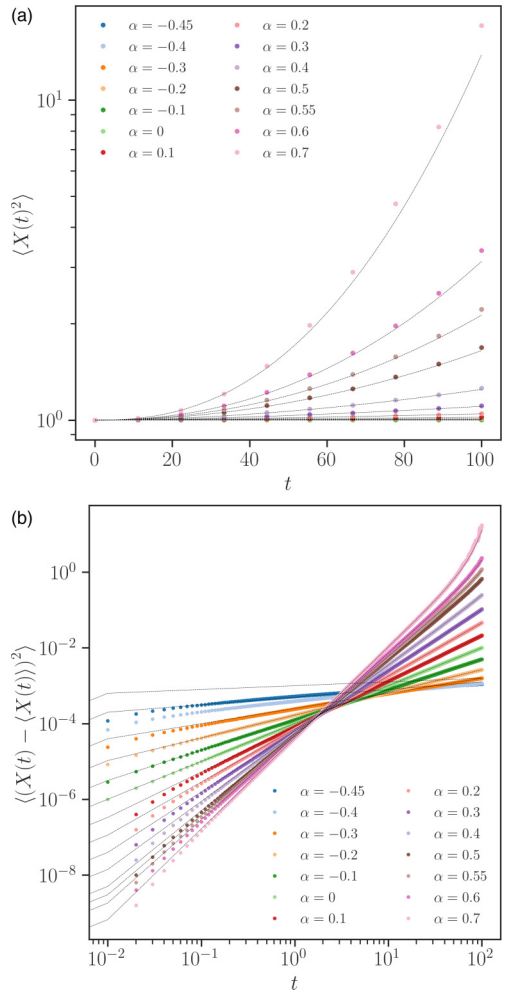

FIG. 3. Results of computer simulations for the MSD in log-linear scale (a) and the variance in log-log scale (b) of SGBM, with the theoretical predictions (25) and (26) shown as the dashed curves for each α (correspondingly, in each panel). The values of exponent α implemented are given in the legend. Parameters: the volatility magnitude is $\sigma_\alpha = 10^{-2}$ (given without units here), the drift is absent $\mu = 0$, the elementary time step for the lag time is $\delta\Delta = 10^{-2}$, the trajectory length is $T = 10^2$, and the number of independent trajectories used for final ensemble averaging is $N = 5 \times 10^4$.

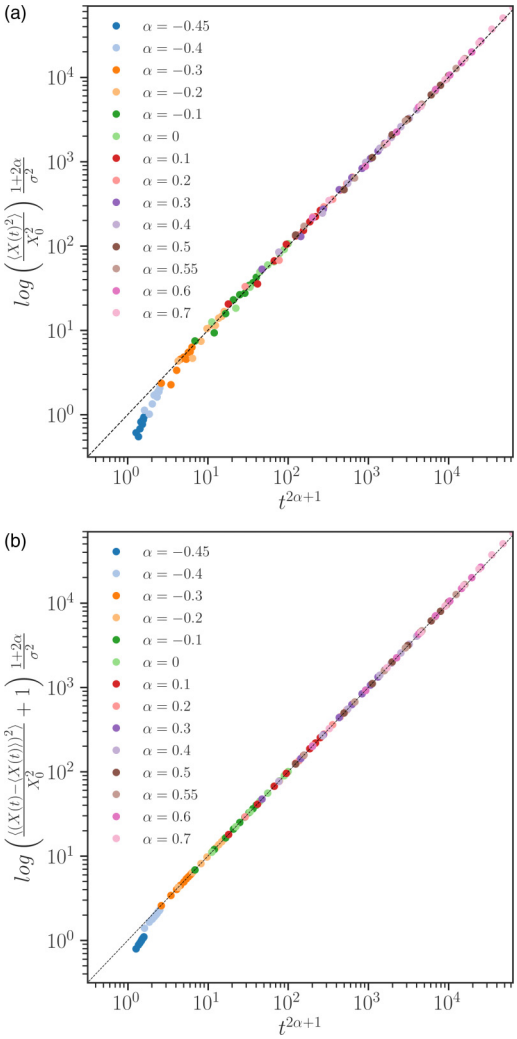

FIG. 4. Results of computer simulations for the rescaled MSD of SGBM, computed as $\log\left[\frac{\langle X^2_{\mathrm{SGBM}}(t)\rangle}{[X(0)]^2}\right]\frac{2\alpha+1}{\sigma_\alpha^2}$, are shown in panel (a), while those for the behavior of the rescaled variance, evaluated as $\log\left\{\frac{\langle [X_{\mathrm{SGBM}}(t) - \langle X_{\mathrm{SGBM}}(t)\rangle]^2\rangle}{[X(0)]^2} + 1\right\}\frac{2\alpha+1}{\sigma_\alpha^2}$, are illustrated in panel (b). The diagonal dotted black lines in both panels correspond to the theoretical predictions (25) and (26), correspondingly. Parameters are the same as in Fig. 3, with the same color scheme for varying values of α exponent.

With the Euler-Murayama scheme [23], a stochastic differential equation of the form

$$dX(t) = f(X(t))dt + g(X(t))dW(t), \tag{52}$$

subject to the initial condition $X(0) = X(t = 0)$, can be solved in an interval $[0, T]$ via splitting into $\bar{N}$ time steps

$$0 = t_0 < t_1 < t_2 < \ldots < t_{\bar{N}} = T \tag{53}$$

or $t_i = t_0 + i \times \Delta t$ with

$$\Delta t = T/\bar{N}. \tag{54}$$

Applying the discrete scheme to Eq. (52), with the increments

$$\Delta W_n = W(t_{n+1}) - W(t_n), \tag{55}$$

the recurrent relation to generate SGBM trajectories [consistent with the Îto interpretation] becomes

$$X_{n+1} = X_n + \mu X_n \Delta t + \sigma(t_n) X_n \times \Delta W_n. \tag{56}$$

B. Description of the results of simulations

The results of computer simulations of Eq. (6) reveal good-to-excellent agreement with the theoretical predictions. First, the MSD of SGBM features a super- and subexponential growth in time for the volatility exponents in the range $\alpha > 0$ and $-1/2 < \alpha < 0$, respectively, see Figs. 3 and 4. This growth is in good agreement with theoretical prediction (25). This agreement and the precise scaling of the spreading dynamics is clearly visible when presenting the data in terms of the rescaled MSD and the variance, namely

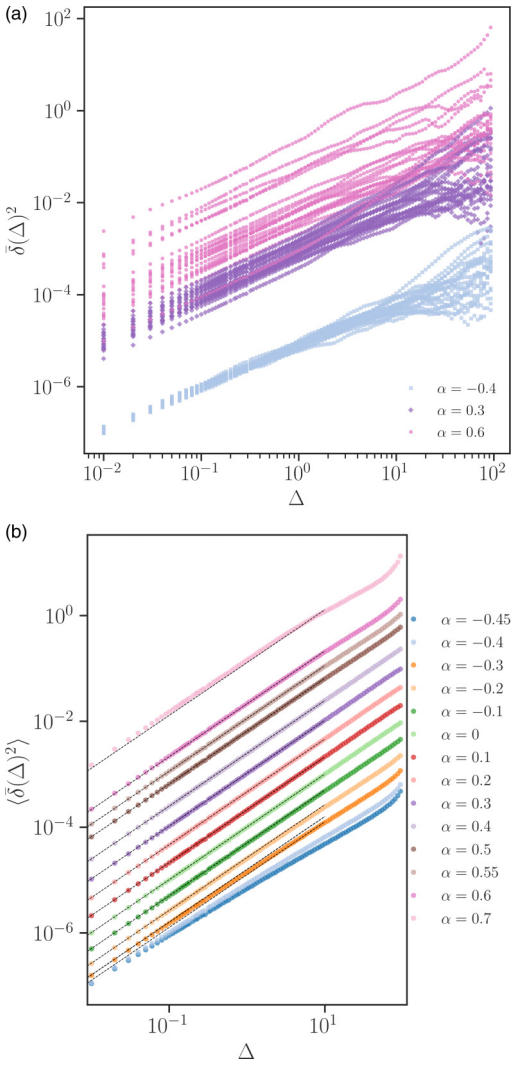

FIG. 5. Distribution of individual TAMSDs for $\alpha = \{-0.4, 0.3, 0.6\}$ in log-log scale (a) and the computed evolution of the mean TAMSDs after averaging over $N = 5 \times 10^4$ SGBM trajectories (for each α value listed in the legend). The dashed lines in panel (b) are the theoretical short-lag-time asymptotes (32). Parameters are the same as in Fig. 3.

as $\log\left[\frac{\langle X^2_{\mathrm{SGBM}}(t)\rangle}{[X(0)]^2}\right]\frac{2\alpha+1}{\sigma_0^2}$ and $\log\left\{\frac{\langle[X_{\mathrm{SGBM}}(t)-\langle X_{\mathrm{SGBM}}(t)\rangle]^2\rangle}{[X(0)]^2}+1\right\}\frac{2\alpha+1}{\sigma_0^2}$, versus the rescaled time $t^{2\alpha+1}$, as shown in Fig. 4 in log-log scale. The theoretical asymptotes (25) and (26) are simply the diagonals in both panels of Fig. 4, excellently coinciding with the results of simulations. Note that the initial point—the first simulation step δt—is not shown in Fig. 3 for larger positive values of exponent α. As the values of $\sigma(\delta t)$ for such α values are very small, the MSD cannot be presented adequately in log-log scale.

The magnitude of the MSD of SGBM computed at the last point of the trajectory for varying α values reveals a *nonmonotonic* dependence on α, with a minimum at $\alpha_{\min} \approx -0.39$ for the trajectories with length $T = 100$, as shown in Fig. 9. This value follows from minimizing (25) over α that yields

$$\alpha_{\min} = \frac{1 - \log T}{2 \log T}, \tag{57}$$

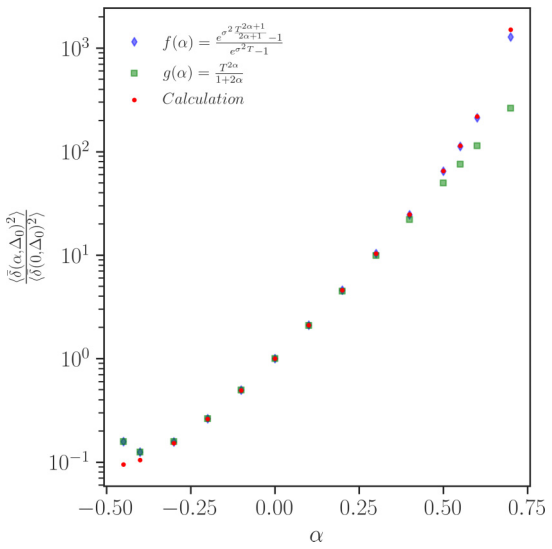

FIG. 6. The same as in Fig. 2, but obtained from computer simulations of SGBM (red circles). Theoretical expectation (47) and its simplistic form (49) are denoted in the legend and reveal excellent agreement with the simulation data for moderate magnitudes of $|\alpha|$. Parameters are the same as in Fig. 3 and $\Delta_0 = 5$ elementary time steps (or time equal to 0.05).

that for long trajectories at $T \to \infty$ approaches the natural value $\alpha_{\min} \to -1/2$ for the slowest-dynamics state of SGBMs. Note that for exponents α near the "boundary" $\alpha = -1/2$ the agreement of the MSD and the variance from simulations versus theory is not that great. The reason for this disparity can be a finite—and, to a certain extent, arbitrary—volatility value used in simulations at the very first time step, see also the results of this analysis presented in Fig. 10.

Second, the distribution of individual TAMSD realizations for varying values of the volatility exponent are shown in Fig. 5(a). As intuitively expected, the spread of TAMSDs with respect to their mean TAMSDs is larger for more superexponential MSDs of SGBM, i.e., as the scaling exponent $\alpha > 0$ increases. In contrast, for negative values of α the TAMSD realizations become more reproducible and the respective spread shrinks. A detailed evaluation of the ergodicity breaking parameter [49,54]

$$\mathrm{EB}(\Delta) = \langle(\overline{\delta^2(\Delta)})^2\rangle \big/ \langle\overline{\delta^2(\Delta)}\rangle^2 - 1 \tag{58}$$

for GBM and SGBM deserves a separate investigation [55]. The mean TAMSDs for varying exponents scale linearly in the region of short lag times, with the TAMSD-to-MSD proportionality relation (33) satisfied, see Fig. 5(b).

Here, again, for the most negative scaling exponents in the set the TAMSD magnitudes from simulations do not exactly match with theoretical predictions in part because of a finite volatility used in the numeric scheme at the initial time step. The effect of this value [used to approximate the diverging magnitude of $\sigma(t = 0)$] is examined in Fig. 10. For the exponent $\alpha = -0.45$, for volatility magnitude $\sigma_0 = 10^{-2}$ and time step $\Delta t = 10^{-2}$ the time-initial volatility value is set in Fig. 10 to

$$\sigma_{\mathrm{approx}} \approx 0.1. \tag{59}$$

Since $\sigma(0)$ diverges for $\alpha < 0$ (see also Ref. [19]), to remove this discontinuity, we approximate

$$\sigma(0) = \sigma_{\text{approx}} \tag{60}$$

for all $\alpha < 0$ values. For later time steps, the volatility follows the standard dependence (2). For $\alpha > 0$ we put $\sigma(0) = 0$ in simulations so that the process does not change during the first time step [as visible from Fig. 3(b) where at these conditions the data for the initial timestep is not shown].

Last, the variation of the ratio of mean TAMSDs for SGBM and GBM computed at short lag times with the exponent α is roughly consistent with expression (47) and simple relation (49) (in the region of its applicability). The ratio $\langle\overline{\delta^2_{\text{SGBM}}(\Delta)}\rangle/\langle\overline{\delta^2_{\text{GBM}}(\Delta)}\rangle$ computed at short lag times depends only on the trajectory length and the value of the scaling exponent α, as demonstrated in Fig. 6. We observe that the theoretical asymptote (47) is valid for all values $\alpha \gtrsim -1/2$, while [as expected in virtue of condition (48)] simplistic scaling (49) starts to deviate from the results of simulations for $\langle\overline{\delta^2_{\text{SGBM}}(\Delta)}\rangle/\langle\overline{\delta^2_{\text{GBM}}(\Delta)}\rangle$ at short lag times for larger positive values of α.

VI. DISCUSSION AND CONCLUSIONS

To summarize, the MSD and mean TAMSD of SGBM computed analytically, see expressions (25), (33), (42), and (49), are quantitatively supported by the results of our computer simulations is the essence of our main results. Specifically, the MSD for this modified GBM process with a power-law-dependent volatility revealed a sub- and superexponential growth for the scaling exponents in the range $-1/2 < \alpha < 0$ and $\alpha > 0$, respectively. In contrast, the mean TAMSD of SGBM was shown to grow exclusively linearly with the lag time at $\Delta/T \ll 1$, irrespective of volatility decaying or growing in time. For SGBM—the multiplicative-noise stochastic process featuring a deterministic growth or decline of volatility, $\sigma(t)$—the found dependencies for the MSD and mean TAMSD as well as the MSD-to-TAMSD ratio are the same as for the standard GBM process (with a constant volatility) [47,48]. The results of our computer simulations excellently support the predicted theoretical trends for the MSD and mean TAMSD of such SGBM.

Note that, although SGBM does not require the condition (23) per se, a "critical point" at $\alpha \to -1/2$ does exist if one sets $t \to 0$ as the lower limit of integration in the expression (21). The model of a power-law volatility can, however, be used in a finite range of times, e.g., in a domain where such volatility variations are detected in real financial data [37–39]. Doing so, the initial time can be chosen $t \neq 0$ and the final time T in Eq. (21) stays finite, so does the volatility magnitude. Physically, the MSD slows down its growth with time at $\alpha \to -1/2$ and ultimately stagnates. At this point, and also for smaller negative α, the MSD ceases to have exponential growth typical of GBM. We thus limit the analysis by $\alpha > -1/2$, focusing more on SGBM with a faster-than-exponential growth, at the region $\alpha > 0$. Under such conditions, additionally, no regularization of the initial volatility (60) is necessary in simulations and, thus, their results can be compared to the theory quantitatively.

We stress that the approach to $\alpha = -1/2$ in terms of the functional dependence of the MSD (and mean TAMSD) on time can be intricate. A similar situation was observed, e.g., for SBM with a diffusivity of the form (3) as the SBM exponent $\bar{\alpha} \to 0$. In this case, the MSD changes its dependence from the standard $\sim t^{\bar{\alpha}}$ for SBM to a much slower, $\sim \log[t]$-like growth at long times for this "critical" diffusion process, yielding ultraslow SBM [43]. The question of how exactly the MSD and TAMSD of SGBM change their functional dependencies in time as $\alpha \to -1/2$ deserves a separate future analysis.

From the point of view of the description of real financial data based on GBM and SGBM, the current results for SGBM (with a linear growth of the mean TAMSD with lag time) indicate that deterministic variations of volatility in time get reflected only in the *magnitude* of mean TAMSD but not in its functional dependence on the lag time. Therefore, the TAMSD linearity for a given financial time series is not a good indicator of validity of standard GBM as the underlying stochastic process, as compared to SGBM.

Finally, as possible future developments of the SGBM model some resetting approaches [56–58], ageing- and delay-time-based analyses of the TAMSD [47,48], and GBM-SGBM under regulations or constraints can be possible. The volatility that depends *both* on time and actual price as power laws [see Eq. (1)], namely

$$\sigma(X,t) \sim t^{\alpha} X^{\gamma}, \tag{61}$$

can also be used as a generalization of SGBM. Its analog in the realm of nonexponential in the MSD anomalous diffusion processes is the diffusion with a power-law-like time- and position-dependent diffusivity [30]. Lastly, the evolution of two SGBM processes—*coupled* via a volatility function $\sigma(X_1, X_2)$ or via correlated noise terms, see, e.g., Ref. [16]—can be used to study mutual effects on the dynamics of *interlinked options* or stocks [for instance, in application to performance- and portfolio-optimization tasks].

ACKNOWLEDGMENTS

A.G.C. is grateful to Humboldt University of Berlin for hospitality and support. The authors thank F. Thiel for helping with integrals (37) and (38). R.M. acknowledges financial support by the Deutsche Forschungsgemeinschaft (DFG Grants No. ME 1535/7-1 and No. ME 1535/12-1). R.M. also thanks the Foundation for Polish Science (Fundacja na rzecz Nauki Polskiej) for support within an Alexander von Humboldt Polish Honorary Research Scholarship.

APPENDIX A: SUPPLEMENTARY FIGURES

Here we present some auxiliary figures supporting the claims in the main text, see Figs. 7–10.

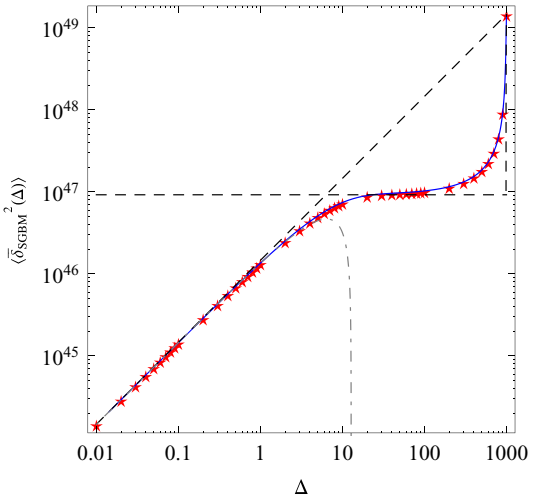

FIG. 7. The same as in Fig. 1 but for $\alpha = 0.2$. The short-lag-time asymptote (32), the long-lag-time mean TAMSD expansion (46), and the intermediate-lag-time plateau of the TAMSD (45) are shown as the dashed curves. The results of numerical integration of Eq. (29) are the red stars. The dot-dashed gray curve shows the first two terms in the short-lag-time TAMSD expansion, with a divergence at $\sim\Delta^\star \approx 12.6$. Other parameters are $X(0) = 1$, $T = 10^3$, and $\sigma_\alpha = 10^{-1}$.

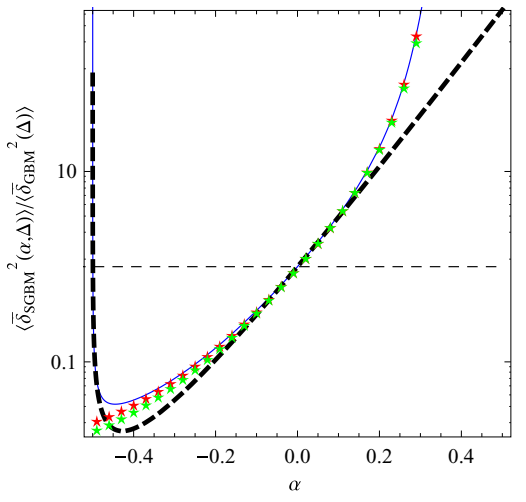

FIG. 8. The same as in Fig. 2, but according to Eq. (B5) for SGBM with the "regularized" volatility of the form (B1), shown as the blue curve. The volatility- and lag-time-independent asymptote (49) is the thick dashed black curve, while the level of unity is the horizontal dashed line. The results of numerical integration of the TAMSD (29) with the averaged-squared volatility (B3) are the red stars (for $\Delta = 1$) and the green stars (for $\Delta = 10^2$). Parameters for the analytical calculations are $T = 10^3$, $\sigma_0 = 10^{-3}$, and $\sigma_\alpha = 10^{-2}$.

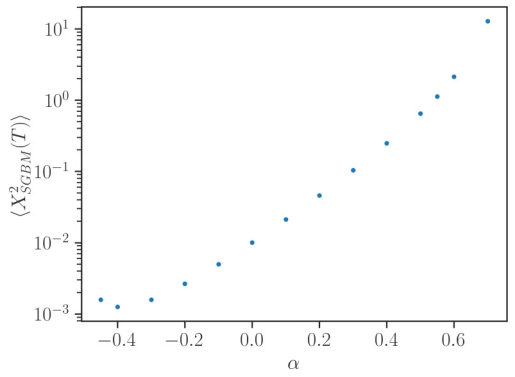

FIG. 9. Magnitude of the MSD of SGBM at the terminal point $t = T$, plotted versus the scaling exponent α, for the parameters of Fig. 3.

APPENDIX B: GENERALIZED TIME-DEPENDENT VOLATILITY

Performing the same MSD and TAMSD calculations for a generalized version of (2), for which the time-dependent term is a correction to the basal volatility σ_0 (more applicable to real financial data [37,39]), namely for

$$\sigma(t) = \sigma_0 + \sigma_\alpha t^\alpha, \tag{B1}$$

one gets for the MSD

$$\left\langle X^2_{\rm SGBM}(t)\right\rangle = [X(0)]^2 e^{2\mu t} e^{\widetilde{\sigma^2(t)}t}, \tag{B2}$$

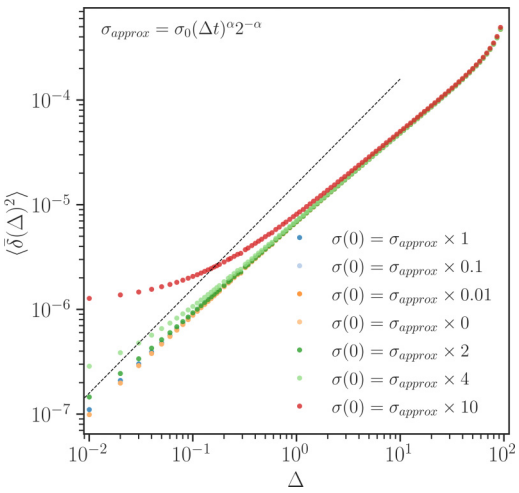

FIG. 10. Variation of the short-lag-time TAMSD of SGBM as obtained from simulations for a varying volatility value at the initial time step, computed for $\alpha = -0.45$ (close to the lower boundary of the exponent) and with $\sigma_{\rm approx}$ given by Eq. (59). The asymptote (32) is the dotted line.

where now

$$\widetilde{\sigma^2(t)} = \sigma_0^2 + 2\sigma_0\sigma_\alpha \frac{t^\alpha}{\alpha+1} + \sigma_\alpha^2 \frac{t^{2\alpha}}{2\alpha+1}. \tag{B3}$$

Expanding the integrand in the TAMSD for short lag times, integrating the first term linear in Δ, and retaining the leading-order term one gets, similarly to (33), that

$$\overline{\langle \delta^2_{\rm SGBM}(\Delta)\rangle} \approx [X(0)]^2 \frac{\Delta}{T}\left[e^{\widetilde{\sigma^2(T)}T} - 1\right] \sim \langle X^2_{\rm SGBM}(T)\rangle \frac{\Delta}{T}. \tag{B4}$$

This proportionality of the mean TAMSD and the MSD seems universal, valid for time-independent [47] and time-varying forms of the volatility. For such SGBM, the ratio of the TAMSDs at short lag times for $\alpha \neq 0$ to that at $\alpha = 0$ is

$$\frac{\overline{\langle \delta^2_{\rm SGBM}(\Delta)\rangle}}{\overline{\langle \delta^2_{\rm GBM}(\Delta)\rangle}} \sim \frac{e^{\widetilde{\sigma^2(T)}T} - 1}{e^{(\sigma_0+\sigma_\alpha)^2 T} - 1}, \tag{B5}$$

where $\widetilde{\sigma^2(T)}$ in (B4) and (B5) is given by (B3). For small σ_0 and not too long trajectories, such that $\sigma_0 \ll \sigma_\alpha T^{2\alpha}$ holds, the ratio (B5) returns the same law (49), see Fig. 8.

For other functional forms of $\sigma(t)$, e.g., for $\sigma(t) = \sigma_0 + \sigma_\omega \sin[\omega t]$, we get $\widetilde{\sigma^2(t)} = \sigma_0^2 + \sigma_\omega^2/2$ so that at short lag times the TAMSD of this modified GBM (MGBM) grows compared to the case $\sigma_\omega = 0$. For $T = 2\pi/\omega$ and $\mu = 0$, using (28) one gets

$$\frac{\overline{\langle \delta^2_{\rm MGBM}(\Delta)\rangle}}{\overline{\langle \delta^2_{\rm GBM}(\Delta)\rangle}} \sim \frac{e^{(\sigma_0^2+\sigma_\omega^2/2)T} - 1}{e^{\sigma_0^2 T} - 1}. \tag{B6}$$

For the exponentially varying volatility, $\sigma_\pm(t) = \sigma_\beta e^{\pm\beta t}$, the MSD grows double-exponentially in time,

$$\langle X^2_{\rm MGBM}(T)\rangle = [X(0)]^2 e^{\widetilde{\sigma^2(T)}T} = [X(0)]^2 e^{\pm\frac{\sigma_\beta^2(e^{\pm 2\beta T}-1)}{2\beta}}, \tag{B7}$$

and the ratio of the short-lag-time mean TAMSD to the MSD is again the universal Δ/T. The ratio of the short-lag-time TAMSDs,

$$\frac{\overline{\langle \delta^2_{\rm MGBM}(\Delta)\rangle}}{\overline{\langle \delta^2_{\rm GBM}(\Delta)\rangle}} \sim \frac{e^{\pm\frac{\sigma_\beta^2(e^{\pm 2\beta T}-1)}{2\beta}} - 1}{e^{\sigma_0^2 T} - 1}, \tag{B8}$$

increases with $\beta > 0$ for growing volatilities $\sigma_+(t)$ and it decreases for decreasing volatilities $\sigma_-(t)$.

[1] L. Bachelier, Théorie de la Spéculation, Ann. Ec. Norm. Super. **17**, 21 (1900).

[2] V. Bronzin, *Theorie der Prämiengeschäfte* (Verlag Franz Deticke, Leipzig, 1908).

[3] F. Black and M. Scholes, The pricing of options and corporate liabilities, J. Polit. Econ. **81**, 637 (1973).

[4] R. C. Merton, Theory of rational option pricing, Bell J. Econ. Manag. Sci. **4**, 141 (1973).

[5] R. C. Merton, Option pricing when underlying stock returns are discontinuous, J. Financ. Econ. **3**, 125 (1976).

[6] B. Oksendal, *Stochastic Differential Equations*, 6th ed., (Springer, Berlin, 2005).

[7] I. Karatzas and S. E. Shreve, *Brownian Motion and Stochastic Calculus* (Springer-Verlag, New York, 1988).

[8] R. N. Mantegna and H. E. Stanley, *An Introduction to Econophysics: Correlations and Complexity in Finance* (Cambridge University Press, Cambridge, UK, 2000).

[9] J.-P. Bouchaud and M. Potters, *Theory of Financial Risk and Derivative Pricing: From Statistical Physics to Risk Management* (Cambridge University Press, Cambridge, UK, 2000).

[10] J.-P. Fouque, G. Papanicolaou, and K. R. Sircar, *Derivative in Financial Markets with Stochastic Volatility* (Cambridge University Press, Cambridge, UK, 2000).

[11] M. Yor, *Exponential Functionals of Brownian Motion and Related Processes* (Springer-Verlag, Germany, 2001).

[12] S. L. Heston, A closed-form solution for options with stochastic volatility with applications to bond and currency options, Rev. Finan. Stud. **6**, 327 (1993).

[13] A. A. Dragulescu and V. M. Yakovenko, Probability distribution of returns in the Heston model with stochastic volatility, Quant. Finance **2**, 443 (2002).

[14] S. G. Kou, A jump-diffusion model for option pricing, Manag. Sci. **48**, 955 (2002).

[15] O. E. Barndorff-Nielsen, Normal inverse Gaussian distributions and stochastic volatility modelling, Scand. J. Stat. **24**, 1 (1997).

[16] O. E. Euch and M. Rosenbaum, The characteristic function of rough Heston models, Math. Finance **29**, 3 (2019).

[17] F. Black, Studies of stock price volatility changes, in *Proceedings of the 1976 Meetings of the American Statistics Association* (American Statistical Association, Washington DC, USA, 1976), pp. 177–181.

[18] J. C. Cox and S. A. Ross, The valuation of options for alternative stochastic processes, J. Finan. Econ. **3**, 145 (1976).

[19] P. P. Boyle and Y. Tian, Pricing lookback and barrier options under the CEV process, J. Finan. Quant. Anal. **34**, 241 (1999).

[20] J. Cox, Notes on Option Pricing I: Constant Elasticity of Variance Diffusions, Working paper, Stanford University (1975) reprinted in [J. Portfolio Manag. **23**, 15 (1996)].

[21] D. Emanuel and J. MacBeth, Further results on the constant elasticity of variance call option pricing model, J. Financ. Quant. Anal. **17**, 533 (1982).

[22] D. Davydov and V. Linetsky, Pricing and hedging path-dependent options under the CEV process, Manage. Sci. **47**, 949 (2001).

[23] M. R. R. Tabar, *Analysis and Data-Based Reconstruction of Complex Nonlinear Dynamical Systems* (Springer Nature Switzerland AG, Cham, 2019).

[24] M. Magdziarz, Black-Scholes formula in subdiffusive regime, J. Stat. Phys. **136**, 553 (2009).

[25] S. Orzel and A. Weron, Calibration of the subdiffusive Black-Scholes model, Acta Phys. Polon. B **41**, 1151 (2010).

[26] G. Krzyzanowski and M. Magdziarz, A computational weighted finite difference method for American and barrier options in

subdiffusive Black-Scholes model, Comm. Nonlin. Sci. Numer. Simul. **96**, 105676 (2021).

[27] F. Biagini, Y. Hu, B. Oksendal, and T. Zhang, *Stochastic Calculus for Fractional Brownian Motion and Applications* (Springer Science + Business Media, New York, 2008), Chap. 7.

[28] A. W. C. Lau and T. C. Lubensky, State-dependent diffusion: Thermodynamic consistency and its path integral formulation, Phys. Rev. E **76**, 011123 (2007).

[29] A. G. Cherstvy, A. V. Chechkin, and R. Metzler, Anomalous diffusion and ergodicity breaking in heterogeneous diffusion processes, New J. Phys. **15**, 083039 (2013).

[30] A. G. Cherstvy and R. Metzler, Ergodicity breaking, ageing, and confinement in generalized diffusion processes with position and time dependent diffusivity, J. Stat. Mech. (2015) P05010.

[31] T. Sandev, A. Schulz, H. Kantz, and A. Iomin, Heterogeneous diffusion in comb and fractal grid structures, Chaos Soliton. Fract. **114**, 551 (2018).

[32] X. Wang, W. Deng, and Y. Chen, Ergodic properties of heterogeneous diffusion processes in a potential well, J. Chem. Phys. **150**, 164121 (2019).

[33] W. Wang, A. G. Cherstvy, X. Liu, and R. Metzler, Anomalous diffusion and nonergodicity for heterogeneous diffusion processes with fractional Gaussian noise, Phys. Rev. E **102**, 012146 (2020).

[34] B. Dupire, Pricing with a smile, Risk **7**, 18 (1994).

[35] B. Dumas, J. Fleming, and R. E. Whaley, Implied volatility functions: Empirical tests, J. Finance **53**, 2059 (1998).

[36] A. Carbone, G. Castelli, and H. E. Stanley, Time-dependent Hurst exponent in financial time series, Physica A **344**, 267 (2004).

[37] K. E. Bassler, J. L. McCauley, and G. H. Gunaratne, Nonstationary increments, scaling distributions, and variable diffusion processes in financial markets, Proc. Natl. Acad. Sci. U.S.A. **104**, 17287 (2007).

[38] L. Seemann, J. L. McCauley, and G. H. Gunaratne, Intraday volatility and scaling in high frequency foreign exchange markets, Intl. Rev. Fin. Anal. **20**, 121 (2011).

[39] L. Seemann, J.-C. Hua, J. L. McCauley, and G. H. Gunaratne, Ensemble vs. time averages in financial time series analysis, Physica A **391**, 6024 (2012).

[40] S. C. Lim and S. V. Muniandy, Self-similar Gaussian processes for modeling anomalous diffusion, Phys. Rev. E **66**, 021114 (2002).

[41] F. Thiel and I. M. Sokolov, Scaled Brownian motion as a mean-field model for continuous-time random walks, Phys. Rev. E **89**, 012115 (2014).

[42] J.-H. Jeon, A. V. Chechkin, and R. Metzler, Scaled Brownian motion: A paradoxical process with a time dependent diffusivity for the description of anomalous diffusion, Phys. Chem. Chem. Phys. **16**, 15811 (2014).

[43] A. Bodrova, A. V. Chechkin, A. G. Cherstvy, and R. Metzler, Ultraslow scaled Brownian motion, New J. Phys. **17**, 063038 (2015).

[44] H. Safdari, A. G. Cherstvy, A. V. Chechkin, F. Thiel, I. M. Sokolov, and R. Metzler, Quantifying the non-ergodicity of scaled Brownian motion, J. Phys. A **48**, 375002 (2015).

[45] A. G. Cherstvy and R. Metzler, Anomalous diffusion in time-fluctuating non-stationary diffusivity landscapes, Phys. Chem. Chem. Phys. **18**, 23840 (2016).

[46] A. G. Cherstvy, H. Safdari, and R. Metzler, Anomalous diffusion, nonergodicity, and ageing for exponentially and logarithmically time-dependent diffusivity: Striking differences for massive versus massless particles, J. Phys. D **54**, 195401 (2021).

[47] A. G. Cherstvy, D. Vinod, E. Aghion, A. V. Chechkin, and R. Metzler, Time averaging, ageing and delay analysis of financial time series, New J. Phys. **19**, 063045 (2017).

[48] S. Ritschel, A. G. Cherstvy, and R. Metzler, Universality of delay-time averages for financial time series: analytical results, computer simulations, and analysis of historical stock-market prices (unpublished).

[49] R. Metzler, J.-H. Jeon, A. G. Cherstvy, and E. Barkai, Anomalous diffusion models and their properties: non-stationarity, non-ergodicity, and ageing at the centenary of single particle tracking, Phys. Chem. Chem. Phys. **16**, 24128 (2014).

[50] J. L. McCauley, Time vs. ensemble averages for nonstationary time series, Physica A **387**, 5518 (2008).

[51] O. Peters and W. Klein, Ergodicity Breaking in Geometric Brownian Motion, Phys. Rev. Lett. **110**, 100603 (2013).

[52] O. Peters, The ergodicity problem in economics, Nat. Phys. **15**, 1216 (2019).

[53] F. Thiel (private communication, 2021).

[54] Y. He, S. Burov, R. Metzler, and E. Barkai, Random Time-scale invariant diffusion and transport coefficients, Phys. Rev. Lett. **101**, 058101 (2008).

[55] A. G. Cherstvy *et al.*, Ergodicity breaking for geometric Brownian motion (unpublished).

[56] D. Vinod, A. G. Cherstvy, I. M. Sokolov, and R. Metzler, Resetting, time-averaging, and nonergodicity for geometric Brownian motion (unpublished).

[57] V. Stojkoski, T. Sandev, L. Kocarev, and A. Pal, Geometric Brownian motion under stochastic resetting: A stationary yet non-ergodic process, arXiv:2104.01571 (2021).

[58] W. Wang, A. G. Cherstvy, H. Kantz, R. Metzler, and I. M. Sokolov, Time-averaging and emerging nonergodicity upon resetting of fractional Brownian motion and heterogeneous diffusion processes (unpublished). https://doi.org/10.1101/2021.04.28.441681